Acta Crystallographica Section C
Crystal Structure Communications
ISSN 0108-2701

Supramolecular interaction patterns in the zinc(II) dichloride and tin(IV) tetrachloride complexes with dipyrido[*f*,*h*]quinoxaline-6,7-dicarbonitrile

Leonid Kozlov and Israel Goldberg*

School of Chemistry, Sackler Faculty of Exact Sciences, Tel-Aviv University, Ramat-Aviv, 69978 Tel-Aviv, Israel
Correspondence e-mail: goldberg@post.tau.ac.il

Received 15 January 2008
Accepted 28 January 2008
Online 9 February 2008

This study characterizes the supramolecular synthons that dominate the intermolecular organization of the title compounds, namely dichloridobis(dipyrido[*f*,*h*]quinoxaline-6,7-dicarbonitrile)zinc(II), [ZnCl$_2$(C$_{16}$H$_6$N$_6$)$_2$], (I), and tetrachlorido(dipyrido[*f*,*h*]quinoxaline-6,7-dicarbonitrile)tin(IV), [SnCl$_4$(C$_{16}$H$_6$N$_6$)], (II), in their respective crystal structures. Molecules of (I) are located on 2^b axes of rotational symmetry. Their crystal packing is stabilized mostly by π–π stacking and dipole–dipole attractions between the organic ligand fragments of inversion-related neighbouring species, as well as by weak intermolecular C—H$\cdots$N hydrogen bonds. On the other hand, Cl$\cdots\pi$ and N$\cdots\pi$ interactions seem to direct the crystal packing in (II), which is unusual in the sense that its aromatic fragments are not involved in π–π stacking. Molecules of (II) are located on m^b planes of mirror symmetry. This study confirms the diverse structural chemistry of this organic ligand, which can be involved in a wide range of supramolecular interactions. These include effective coordination to various metal ions *via* the phenathroline N-atom sites, π–π stacking and $\pi\cdots$halogen contacts through its extended π-system, and hydrogen bonding and N$\cdots\pi$ interactions through its nitrile groups. The competing natures of the latter make it difficult to predict *a priori* the preferred supramolecular motif that may form in a given structure.

Comment

The phenanthroline-based dipyrido[*f*,*h*]quinoxaline-6,7-dicarbonitrile (DICNQ) ligand has an extended π-electron system and multiple N-atom sites, which make it an attractive reagent in diverse applications. It has been widely used as a multidentate coordination ligand in the synthesis of various transition metal complexes (Liu *et al.*, 2001; Xu *et al.*, 2002; Stephenson & Hardie, 2006). It has also been employed as an efficient antenna chromophore in the design of photonic and biochemical sensors (van der Tol *et al.*, 1998; Arounaguiri & Maiya, 1999; Ambroise & Maiya, 2000). The redox chemistry of Ru$^{\rm I}$ complexes of DICNQ has also been investigated (Kulkarni *et al.*, 2004). We were also interested in exploring the supramolecular reactivity of DICNQ, by evaluating its preferred modes of intermolecular organization as a free ligand or in various complexes with metal ions. To this end, we synthesized DICNQ according to literature procedures (van der Tol *et al.*, 1998; Arounaguiri & Maiya, 1999), determined its crystal structure, and characterized its remarkable π–π stacking as a dominant intermolecular interaction in the solid phase (Kozlov *et al.*, 2008). We report here the crystal structures of the 2:1 complex of DICNQ with zinc(II) dichloride, (I), and the 1:1 complex of DICNQ with tin(IV) tetrachloride, (II), with an emphasis on their supramolecular self-organization and descriptions of the interaction synthons that operate therein.

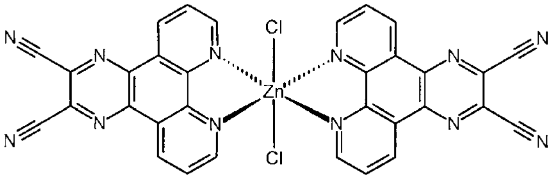

(I)

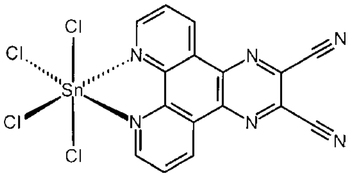

(II)

Representations of (I) and (II) are shown in Fig. 1. In (I), molecules of the complex are located on axes of twofold rotation and the two DICNQ ligands bound to the Zn$^{\rm II}$ ion are symmetry equivalent. In (II), the complex resides on a mirror plane, which is perpendicular to the plane of the ligand. The DICNQ framework is aromatic and is quite planar in the two structures. For the 18-membered delocalized system (excluding the two cyano substituents), the deviations of the individual atoms from their mean plane do not exceed ±0.06 Å (r.m.s. 0.03 Å) in (I) and 0.05 Å (r.m.s. 0.03 Å) in (II). In both structures, the cyano groups deviate to a minor extent from the mean plane of the corresponding aromatic fragment.

The overall topology of complex (I) is dictated by the preferred tetrahedral coordination environment of the Zn$^{\rm II}$ ion with respect to the four ligating species, with the chloride anions occupying two vertices of the tetrahedron. Along the other two directions, the Zn$^{\rm II}$ ion is coordinated in a chelating manner by the phenanthroline side of two rotation-related DICNQ ligands. If the N-atom sites of the coordinated phenanthroline moieties are counted as separate ligands, the coordination environment around the Zn$^{\rm II}$ ion can be described alternatively as a distorted octahedron. No metal coordination by the cyano sites is observed.

doi:10.1107/S010827010800303X

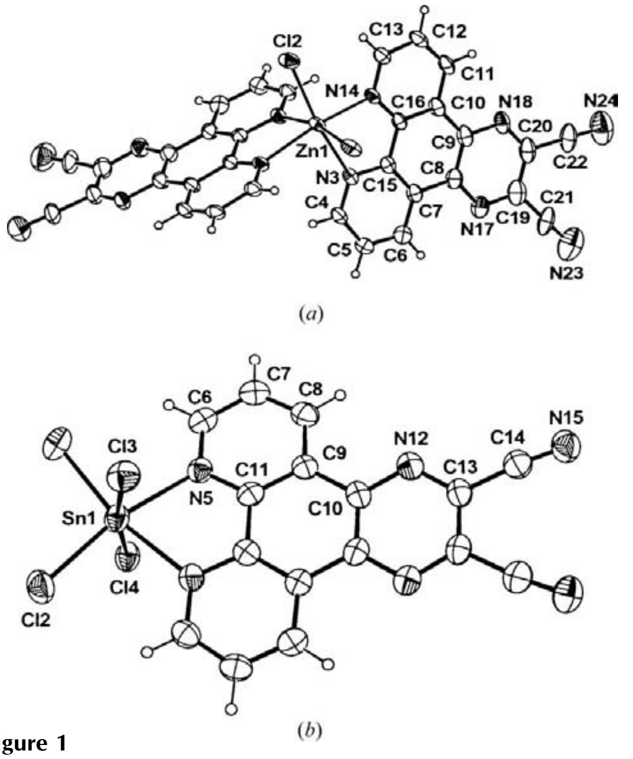

(*a*)

(*b*)

Figure 1
The molecular structures of the title compounds, showing the atom-labelling schemes. Displacement ellipsoids are drawn at the 50% probability level at *ca* 110 K, and H atoms are shown as small spheres of arbitrary radii. (*a*) Compound (I), which is located on the twofold rotation axis at $(1, y, \frac{3}{4})$ passing through the $\mathrm{Zn^{II}}$ ion; only atoms of the asymmetric unit are labelled. (*b*) Compound (II), with atoms of the asymmetric unit labelled. The entire molecule of the complex is located on a plane of mirror symmetry $(x, \frac{1}{4}, z)$, which passes through the $\mathrm{Sn^{IV}}$ ion and is perpendicular to the plane of the DICNQ ligand.

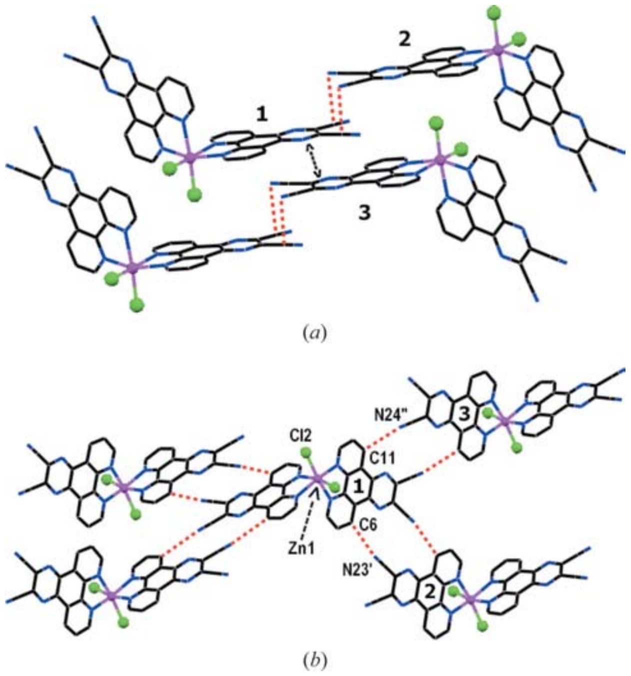

(*a*)

(*b*)

Figure 2
(*a*) The π–π stacking and dipole–dipole interaction modes in (I). The DICNQ fragment labelled (1) is at the symmetry position (x, y, z), that labelled (2) is at $(1 - x, -y, 1 - z)$ and that labelled (3) is at $(\frac{3}{2} - x, \frac{1}{2} - y, 1 - z)$. The predominantly dipole–dipole interactions are indicated by dotted lines, while the π–π stacking is indicated by a double-headed arrow. (*b*) The intermolecular hydrogen-bonding scheme (dotted lines) in (I). The DICNQ fragment labelled (1) is at the symmetry position (x, y, z), that labelled (2) is at $(2 - x, -y, 1 - z)$ and that labelled (3) is at $(\frac{1}{2} - x, \frac{1}{2} - y, 1 - z)$. Zn and Cl atoms are denoted by small spheres. H atoms have been omitted for clarity. Primed atom N23′ is at symmetry position (2) and doubly primed atom N24″ is at symmetry position (3).

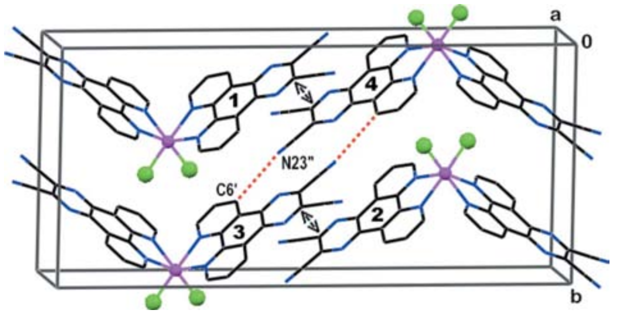

Figure 3
The unit-cell contents in (I), showing some of the supramolecular interactions. The DICNQ fragment labelled (1) is at the symmetry position (x, y, z), that labelled (2) is at $(1 - x, 1 - y, 1 - z)$, that labelled (3) is at $(x - \frac{1}{2}, y + \frac{1}{2}, z)$ and that labelled (4) is at $(\frac{3}{2} - x, \frac{1}{2} - y, 1 - z)$. The weak hydrogen bonds from primed atom C6′ at $(x - \frac{1}{2}, y + \frac{1}{2}, z)$ to doubly primed atom N23″ at $(\frac{3}{2} - x, \frac{1}{2} - y, 1 - z)$ and its inversion-related counterpart are indicated by dotted lines. The π–π stacking interactions between overlapping DICNQ fragments are indicated by arrows. Zn and Cl atoms are denoted by small spheres. H atoms have been omitted for clarity.

It appears that the intermolecular organization in the condensed solid phase of the species thus formed cannot be optimized solely by π–π stacking as in the crystal structure of the free flat DICNQ ligand (Kozlov *et al.*, 2008). Instead, in (I), three different types of specific interactions (in addition to common dispersion) operate in concert. Fig. 2(*a*) illustrates the π–π stacking and dipole–dipole interactions beween DICNQ fragments related to one another by centres of inversion. Thus, significant overlap occurs between the quinoxaline groups related by the symmetry operator $(\frac{3}{4} - x, \frac{1}{2} - y, 1 - z)$ (in the centre of Fig. 2*a*). The relatively short interplanar distance between the corresponding fragments (C8/C9/N17/C19–C22) is 3.29 (1) Å, which is indicative of a strong π–π interaction. In addition, dipolar attractions operate between the cyano groups of DICNQ residues interrelated by inversion at $(\frac{1}{2} - x, -y, \frac{1}{2} - z)$. The distance between the antiparallel pairs of CN dipoles of the two molecules is 3.123 (4) Å, which reflects a rather strong interaction. Preliminary density functional theory calculations (*GAUSSIAN98*; Frisch *et al.*, 1998) confirm the attractive nature of the π–π and dipole–dipole interactions. The third component of the supramolecular interaction in this structure is shown in Fig. 2(*b*). It involves weak C—H$\cdots$N(cyano) hydrogen bonds (Table 1). Every molecule of complex (I) associates *via* eight such hydrogen bonds to four neighbouring species, yielding an extended supramolecular network that propagates through the crystal structure. The unit cell shown in Fig. 3 partly illustrates the combination of the above-described interaction synthons in the crystal structure of (I). It also shows that the chloride ligands of one complex are oriented perpendicular to

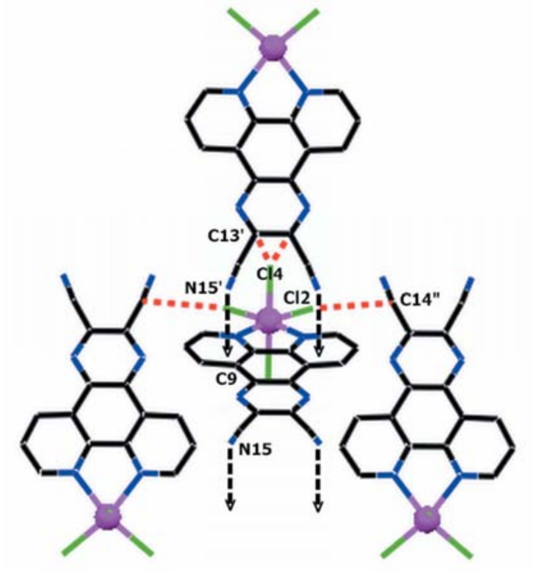

Figure 4
The intermolecular interaction scheme in (II). The Cl$\cdots\pi$ interactions between neighbouring species are indicated by dotted lines. The N$\cdots\pi$ interactions are indicated by dashed arrows. Sn atoms are denoted by small spheres. H atoms have been omitted. Primed atoms are at the symmetry position ($\frac{1}{2}+x, y, -\frac{1}{2}-z$) and doubly primed atoms are at ($\frac{1}{2}-x, \frac{1}{2}+y, \frac{1}{2}+z$).

the π system of adjacent molecules, suggesting the presence of Cl$\cdots\pi$ interactions as well. The observed distance of the chloride anions from the plane of the corresponding DICNQ ring is 3.640 (5) Å, which is, however, considerably longer than expected for a Cl$\cdots\pi$ interaction [Rosokha *et al.*, 2004; see also structure (II) below]. As the π–π stacking and dipole–dipole interactions operate in directions perpendicular to the two DICNQ rings, while the hydrogen bonds operate in different directions parallel to these rings, the entire supramolecular assembly exhibits a three-dimensional connectivity scheme. Structure (I) is nearly isomorphous with the structure of the cobalt dibromide analogue (Stephenson & Hardie, 2006).

The tin tetracholoride complex, (II), is characterized by a distorted octahedral geometry, with the two N atoms of the phenanthroline fragment occupying two adjacent coordination sites of the metal ion (Fig. 1*b*). Somewhat surprisingly, the supramolecular organization of (II) lacks the π–π stacking interactions between aromatic ligands which are often observed in the crystal structures of various metal ions with phenanthroline-type ligands (*e.g.* Bergman *et al.*, 2002; Gut *et al.*, 2002; Gupta *et al.*, 2004; Rubin-Preminger *et al.*, 2008). This may be mainly due to strong attractions between the electron-rich chloride ligand and the electron-deficient areas of the π-electron system in DICNQ. These interactions are illustrated in Fig. 4. They are reflected well in the rather short contact distances, *viz*. Cl4$\cdots$C13($\frac{1}{2}+x, y, -\frac{1}{2}-z$) = 3.254 (3) Å and Cl2$\cdots$C14($\frac{1}{2}-x, \frac{1}{2}+y, \frac{1}{2}+z$) = 3.346 (4) Å, indicative of arrays of significant Cl$\cdots\pi$ interactions that extend in two dimensions, which is consistent with earlier reports (Rosokha *et al.*, 2004). Furthermore, atom Cl4 is located 3.147 (10) Å above the plane of the neighbouring quinoxaline ring [atoms C10/N12/C13 at ($\frac{1}{2}+x, y, -\frac{1}{2}-z$) and ($\frac{1}{2}+x, \frac{1}{2}-y, -\frac{1}{2}-z$)]. Thus, every molecule of the complex is involved in eight such Cl$\cdots\pi$ contacts through its Cl sites ('donating' electrons) and its π system ('accepting' electrons). Fig. 4 also shows that N$\cdots\pi$ interactions provide additional enthalpic stabilization to the observed structure along one direction of the two-dimensional supramolecular array. They involve the C—N groups of one species that interact with the π system of the two pyrido rings of adjacent species. Thus, the observed C9$\cdots$N15($\frac{1}{2}+x, y, -\frac{1}{2}-z$) distance is 3.163 (4) Å, and this N atom is located 3.010 (8) Å above the plane of the corresponding aromatic ring (N5/C6–C9/C11). Each molecule of the complex associates in four such interactions through its pair of cyano groups and the two pyrido rings. The CN bond is not perpendicular to the aromatic ring it overlaps, the approach angle being 46.20 (7)° instead of 90°. Similar CN$\cdots\pi$ interactions were observed earlier in the structure of the octahedral [Ni(DICNQ)$_3$]Br$_2$ complex (Stephenson & Hardie, 2006). The above-described array of intermolecular interactions gives rise to two-dimensional supramolecular motifs. Another observation related to the presence of the N$\cdots\pi$ interactions is the slight inward bending of the cyano groups in (II) compared with the structure of the free DICNQ ligand (Kozlov *et al.*, 2008). The intramolecular N15$\cdots$N15($x, \frac{1}{2}-y, z$) distance is 3.615 (5) Å in (II) compared with 3.999 (6) Å in the structure of the free ligand.

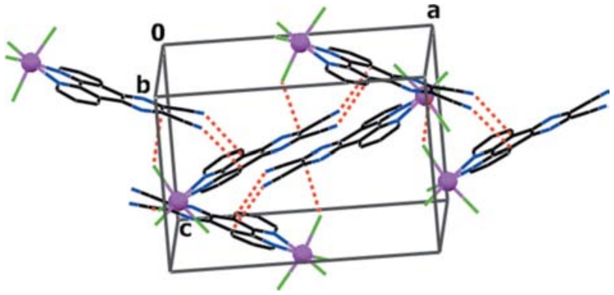

Figure 5
The crystal packing of (II). The Cl$\cdots\pi$ and N$\cdots\pi$ interactions are indicated by dotted lines. Sn atoms are denoted by small spheres. H atoms have been omitted.

In summary, the supramolecular organization in (II) is stabilized mainly by the somewhat less common Cl$\cdots\pi$ and N$\cdots\pi$ interactions in two dimensions, but not by π–π stacking forces like those observed in the structure of DICNQ (Kozlov *et al.*, 2008) and many other complexes of phenanthroline-type ligands (Bergman *et al.*, 2002; Gut *et al.*, 2002; Gupta *et al.*, 2004; Rubin-Preminger *et al.*, 2008).

This study demonstrates the diverse supramolecular reactivity of the DICNQ ligand. The competing natures of the secondary interactions, which involve the extended π system and the nitrile groups, make it difficult to predict *a priori* the preferred supramolecular organization in a given structure.

Experimental

DICNQ was synthesized according to previously reported procedures (Arounaguiri & Maiya, 1999; van der Tol *et al.*, 1998) and was crystallized from ethanol by slow evaporation. For the synthesis of the zinc complex, (I), DICNQ (17.2 mg, 0.06 mmol) was dissolved in hot acetonitrile (15 ml). This solution was mixed with a solution of zinc dichloride (2.9 mg, 0.02 mmol) in boiling acetonitrile (2.5 ml). Slow evaporation of the resulting mixture yielded plate-shaped yellow crystals of (I) after three weeks. For the synthesis of the tin complex, (II), DICNQ (22.8 mg, 0.08 mmol) was dissolved in a hot methanol–ethyl acetate mixture (10 ml, 1:3 *v*/*v*). This solution was mixed with a solution of tin dichloride dihydrate (12.8 mg, 0.06 mmol) in methanol (2.5 ml) under boiling/reflux conditions. Brown needle-shaped crystals of (I) appeared after one month of slow evaporation of the solvent under ambient conditions. It appears that during the preparative process of (II), the Sn^{II} species was oxidized to an Sn^{IV} species, leading to the $SnCl_4$–DICNQ product.

Compound (I)

Crystal data

$[ZnCl_2(C_{16}H_6N_6)_2]$
$M_r = 700.81$
Monoclinic, $C2/c$
$a = 8.3051$ (2) Å
$b = 12.6449$ (3) Å
$c = 28.0176$ (12) Å
$\beta = 97.766$ (2)°

$V = 2915.34$ (16) Å^3
$Z = 4$
Mo $K\alpha$ radiation
$\mu = 1.07$ mm^{-1}
$T = 110$ (2) K
0.40 × 0.20 × 0.15 mm

Data collection

Nonius KappaCCD diffractometer
Absorption correction: multi-scan (Blessing, 1995)
$T_{\min} = 0.673$, $T_{\max} = 0.856$

9284 measured reflections
3433 independent reflections
2501 reflections with $I > 2\sigma(I)$
$R_{\rm int} = 0.035$

Refinement

$R[F^2 > 2\sigma(F^2)] = 0.062$
$wR(F^2) = 0.173$
$S = 1.07$
3433 reflections

213 parameters
H-atom parameters constrained
$\Delta\rho_{\max} = 1.82$ e Å^{-3}
$\Delta\rho_{\min} = -0.52$ e Å^{-3}

Compound (II)

Crystal data

$[SnCl_4(C_{16}H_6N_6)]$
$M_r = 542.77$
Orthorhombic, $Pnma$
$a = 14.8630$ (4) Å
$b = 12.8457$ (3) Å
$c = 9.8852$ (2) Å

$V = 1887.34$ (8) Å^3
$Z = 4$
Mo $K\alpha$ radiation
$\mu = 1.93$ mm^{-1}
$T = 110$ (2) K
0.55 × 0.15 × 0.06 mm

Data collection

Nonius KappaCCD diffractometer
Absorption correction: multi-scan (Blessing, 1995)
$T_{\min} = 0.492$, $T_{\max} = 0.915$

14219 measured reflections
2292 independent reflections
1822 reflections with $I > 2\sigma(I)$
$R_{\rm int} = 0.055$

Refinement

$R[F^2 > 2\sigma(F^2)] = 0.038$
$wR(F^2) = 0.089$
$S = 1.03$
2292 reflections

127 parameters
H-atom parameters constrained
$\Delta\rho_{\max} = 0.53$ e Å^{-3}
$\Delta\rho_{\min} = -0.78$ e Å^{-3}

H atoms bound to C atoms were located in calculated positions and constrained to ride on their parent atoms, with C—H = 0.95 Å and $U_{\rm iso}({\rm H}) = 1.2U_{\rm eq}({\rm C})$. The residual electron-density map of (I) contains a single peak of 1.82 e Å^{-3}, about 2.2 Å from N24, which could not be accounted for. It may be due to a systematic error in the intensity data set (*e.g.* an unnoticed diffraction from ice in the low-temperature experiment).

Table 1
Hydrogen-bond geometry (Å, °) for (I).

D—H···A	D—H	H···A	D···A	D—H···A
C6—H6···N23$^{\rm i}$	0.95	2.61	3.549 (8)	171
C11—H11···N24$^{\rm ii}$	0.95	2.66	3.608 (6)	172

Symmetry codes: (i) $-x + 2, -y, -z + 1$; (ii) $-x + \frac{1}{2}, -y + \frac{1}{2}, -z + 1$.

For both compounds, data collection: *COLLECT* (Nonius, 1999); cell refinement: *DENZO* (Otwinowski & Minor, 1997); data reduction: *DENZO*; program(s) used to solve structure: *SIR97* (Altomare *et al.*, 1994); program(s) used to refine structure: *SHELXL97* (Sheldrick, 2008); molecular graphics: *ORTEPIII* (Burnett & Johnson, 1996) and *Mercury* (Macrae *et al.*, 2006); software used to prepare material for publication: *SHELXL97*.

Supplementary data for this paper are available from the IUCr electronic archives (Reference: LN3086). Services for accessing these data are described at the back of the journal.

References

Altomare, A., Cascarano, G., Giacovazzo, C., Guagliardi, A., Burla, M. C., Polidori, G. & Camalli, M. (1994). *J. Appl. Cryst.* **27**, 435.
Ambroise, A. & Maiya, B. G. (2000). *Inorg. Chem.* **39**, 4264–4272.
Arounaguiri, S. & Maiya, B. G. (1999). *Inorg. Chem.* **38**, 842–843.
Bergman, S. D., Reshef, D., Groysman, S., Goldberg, I. & Kol, M. (2002). *Chem. Commun.* pp. 2374–2375.
Blessing, R. H. (1995). *Acta Cryst.* A**51**, 33–38.
Burnett, M. N. & Johnson, C. K. (1996). *ORTEPIII*. Report ORNL-6895. Oak Ridge National Laboratory, Tennessee, USA.
Frisch, M. J. *et al.* (1998). *GAUSSIAN98*. Revision A.7. Gaussian Inc., Pittsburgh, Pennsylvania, USA.
Gupta, T., Dhar, S., Nethaji, M. & Chakravarty, A. R. (2004). *Dalton Trans.* pp. 1896–1900.
Gut, D., Rudi, A., Kopilov, J., Goldberg, I. & Kol, M. (2002). *J. Am. Chem. Soc.* **124**, 5449–5456.
Kozlov, L., Rubin-Preminger, J. M. & Goldberg, I. (2008). *Acta Cryst.* C**64**, o1–o3.
Kulkarni, M. S., Rao, B. S. M., Sastri, C. V., Maiya, B. G., Mohan, H. & Mittal, J. P. (2004). *J. Photochem. Photobiol. Chem.* **167**, 101–109.
Liu, H., Du, M., Ge, X.-J., Bu, X.-H. & Yang, M. (2001). *Acta Cryst.* E**57**, m100–m102.
Macrae, C. F., Edgington, P. R., McCabe, P., Pidcock, E., Shields, G. P., Taylor, R., Towler, M. & van de Streek, J. (2006). *J. Appl. Cryst.* **39**, 453–457.
Nonius (1999). *COLLECT*. Nonius BV, Delft, The Netherlands.
Otwinowski, Z. & Minor, W. (1997). *Methods in Enzymology*, Vol. 276, *Macromolecular Crystallography*, Part A, edited by C. W. Carter Jr & R. M. Sweet, pp. 307–326. New York: Academic Press.
Rosokha, Y. S., Lindeman, S. V., Rosokha, S. V. & Kochi, J. K. (2004). *Angew. Chem. Int. Ed.* **43**, 4650–4652.
Rubin-Preminger, J. M., Kozlov, L. & Goldberg, I. (2008). *Acta Cryst.* C**64**, m83–m86.
Sheldrick, G. M. (2008). *Acta Cryst.* A**64**, 112–122.
Stephenson, M. D. & Hardie, M. J. (2006). *Cryst. Growth Des.* **6**, 423–432.
Tol, E. B. van der, van Ramesdonk, H. J., Verhoeven, J. W., Steemers, F. J., Kerver, E. G., Verboom, W. & Reinhoudt, D. N. (1998). *Chem. Eur. J.* **4**, 2315–2323.
Xu, Z.-D., Liu, H., Wang, M., Xiao, S.-L., Yang, M. & Bu, X.-H. (2002). *J. Inorg. Biochem.* **92**, 149–155.